



# HHS Public Access

Author manuscript

*IEEE Rev Biomed Eng.* Author manuscript; available in PMC 2015 July 31.

Published in final edited form as:

*IEEE Rev Biomed Eng.* 2014 ; 7: 115–125. doi:10.1109/RBME.2013.2286296.

## A Century of Optocardiography

**B.J. Boukens and I.R. Efimov [Member IEEE]**

Department of Biomedical Engineering, Washington University, St. Louis, 63130 MO USA

I.R. Efimov: Igor@wustl.edu

### Abstract

In the past decade, optical mapping provided crucial mechanistic insight into electromechanical function and the mechanism of ventricular fibrillation. Therefore, to date, optical mapping dominates experimental cardiac electrophysiology. The first cardiac measurements involving optics were done in the early 1900s using the fast cinematograph that later evolved into methods for high-resolution activation and repolarization mapping and stimulation of specific cardiac cell types. The field of “Optocardiography” therefore emerged as the use of light for recording or interfering with cardiac physiology. In this review we discuss how optocardiography developed into the dominant research technique in experimental cardiology. Furthermore, we envision how optocardiographic methods can be used in clinical cardiology.

### Index Terms

Cardiology; conduction; electrophysiology; optical mapping; optogenetics

## I. Introduction

Cardiac electrophysiology enjoyed a long and illustrious history of scientific breakthroughs and clinical advances. The history of electrophysiology goes back to as early as the XVIII century. The desire to understand cardiac electrophysiology resulted in the documentation of the first cardiac action potential by Koelliker and Müller in 1856 and in the first recording of the human electrocardiogram in 1887 by Waller [1, 2]. The clinical importance of these advances is obvious in hindsight, but was not so clear at the time. It is ironic to mention that Waller him-self stated “I do not imagine that electrocardiography is likely to find any very extensive use in the hospital” [1]. The future, however, proved him wrong and for more than 100 years the electrocardiogram and electrical stimulation dominated both clinical and basic cardiac electrophysiology and helped saving millions of human lives.

The field of electrocardiography has evolved from single channel recordings carried out with the Lippmann electrometer to sophisticated modern clinical invasive mapping systems of endocardial and epicardial electrograms or non-invasive electrocardiographic imaging (ECGi) of epicardial electrical activity [3]. These modern electrocardiographic methods guide clinical diagnostics and therapy for life-threatening arrhythmias in millions of patients world-wide [4]. However, electrocardiography faced limitations in experimental and clinical settings such as the inability to record transmembrane potentials, or to record electrograms during and after electric shocks or near the site of stimulation. Also, the spatial resolution is limited by the number and spacing of electrodes. These constraints of electrocardiography

led to a search for different techniques resulting in the development of a field that we deem “optocardiography”.

Optocardiography covers the method of using light to monitor and control cardiac physiology and has evolved over the last century from first cinematographic recordings of a beating frog heart to multiparametric imaging of fluorescence [5, 6]. More recently, development of optogenetics brought a new power to biophotonics permitting not only to record but also to control physiological function [7, 8]. Thus optical methods matched and in some cases exceeded electrical methods in its ability to both control cellular biology and to monitor multiple parameters. The multiparametric nature of biophotonics and its significantly higher spatio-temporal resolution as compared to electrical methods promises to far exceed the power of this modern methodology.

In this review we discuss how optocardiography has evolved from simple observations by the naked eye into sophisticated optical sensing and stimulation methods that may even have exceeded electrocardiography, especially in basic science.

## II. Early history of optical measurements

It was the amazingly innovator Etienne-Jules Marey who at the end of the XIX century did the first experiments that can be considered as the birth of optocardiography. He used the electrometer developed by Lippmann to measure cardiac potentials and used photography to register the electrocardiogram [9]. Later, Marey and his assistant Lucien Bull, developed the “cinematographic gun” that had the shape of a rifle and could be used to monitor wing oscillations of insects and birds in flight [10]. One of the first physiologists that incorporated the Marey-Bull cinematographic method in cardiac research was George Ralph Mines who at that time worked at the Cambridge School of Physiology. Mines was known for crafting his own equipment and devices that he used for his experiments. A century ago, in 1913, he published a study in which he recorded the contraction of the frog heart by taking photographs of the beating organ at fifteen frames per second on bromide paper using the Marey-Bull cinematographic method [11]. Figure 1C shows a sequence of 24 photographs that was displayed in the paper of Mines from 1913. Later, Carl J. Wiggers used the cinematograph to monitor the order of irregular contractions during ventricular fibrillation [12, 13]. Wiggers already realized at that time the advantages of using optics in cardiology: “.noting simultaneously the movements that occur in diverse portions of the ventricular surface..... in addition allows considerable magnification of the quiverings occurring in individual areas of the ventricle.”[12]. Interestingly, the main reason for Wiggers to use cinematography in his experiments is the same reason that we use optical measurements in modern cardiac electrophysiology, namely, the high spatial resolution.

## III. Introduction of fluorescent dyes in optical measurements

In the late 1960s, Larry Cohen attempted to measure the neuronal action potential by using the change in light scattering. He wrote: “We hope that with further improvements in technique it will be possible to sort out the significant parameters more effectively and that the results will provide a useful “new look” at the mechanism of nerve conduction.”[14] We believe this led to the development of optical measuring methods based on the voltage-

dependent characteristics of fluorescent dyes, also called potentiometric dyes [15]. These dyes bind to the cell membrane and exhibit an emission spectrum shift upon a change of the membrane potential. Using the right filter settings, variations in fluorescence can be detected. These variations are linearly related to the change in membrane potential and thereby it is possible to optically measure the action potential (Fig 2a). The proof of this promising technique was given by measuring the action potential of the axon in 1973, the first cardiac application was shown three years later (Fig 2B) [16, 17]. The potentiometric dye that was used in these pioneer experiments was Merocyanine 540. Although the action potential could be measured for hours the signal-to-noise ratio was difficult to maintain throughout the experiment due to washout and photobleaching [18, 19].

The attempt to improve the recording of optical action potentials led to the development and validation of several potentiometric dyes. The most popular ones are styryl dyes like RH-241, di-4-ANEPPS and di-8-ANEPPS because of their low levels of phototoxicity, high emission magnitude and large fractional change of fluorescence during action potential (up to 12%) [20, 21]. The rapid change in fluorescence precedes the micro-electrode signal when measured from the same area [22]. The latter suggests that optical signals are well suited to detect fast cellular electrical activities with time and space resolutions comparable or even superior to those obtained using microelectrode techniques [22].

The majority of the potentiometric dyes has a low excitation/emission wavelength and only allows measurements of superficial tissue layers. This limitation was circumvented by the modifications of styryls dyes that generated a red shift of the excitation and emission spectra [23–26]. The use of these red-shifted dyes allowed for the first time to image deeper anatomical structures in hearts of large mammals, such as man, dog, pig and sheep [27]. Furthermore, these dyes allowed optical recordings from blood-perfused tissue [25]. However, a disadvantage is that intense excitation light can partly photobleach fluorescent dyes and lead to the generation of toxic side products that can damage cardiomyocytes. This process is called phototoxicity and is mainly an issue in thin tissue preparations as the sinus and atrioventricular node, monolayers or single cells [17, 28, 29]. In tissue or whole organ preparations phototoxicity is generally negligible.

## IV. The advantage of high spatial resolution of optical recordings

### A. Epicardial mapping

As mentioned in the introduction, Wiggers already realized in the 1930s that spatial information about the sequence of activation, or activation mapping, is of crucial importance for understanding normal pattern of activation and mechanisms of arrhythmias. The conventional activation mapping studies were done by the use of needle electrodes or multi-electrode grids with an inter-electrode distance not smaller than 300 micrometer. The use of optical action potentials for activation mapping provided an enormous increase in spatial resolution down to 0.1 micrometer inter-pixel-distance. This resolution allowed measuring the detailed activation pattern of the sinus and atrioventricular node during a single beat in the adult heart (Fig 3) [27, 30]. The possibility to reduce the field of view by increasing magnification improved the spatial resolution even more. This enabled Kamino and colleagues to localize pacemaking in the early embryonic heart in 1981 [31]. Next to the

increase in spatial resolution the use of potentiometric dyes also permitted the recording of the activation front after ventricular shock, which was impossible with electrodes due to the enormous stimulus artifact (Fig 4) [32].

In the late 1980s optical action potentials were used to measure conduction velocity in papillary muscle [33]. Later in the early 1990s, the recording of optical action potentials was validated by comparison with computer simulations. This study showed that the maximum of the first and second derivatives of the optical action potentials closely correlated with the activation and repolarizations times in the intact heart [21]. Various studies followed to map the activation pattern of the rabbit, dog and man heart [34]. Not only optical mapping confirmed existing knowledge about activation patterns, it also provided high-resolution data that revealed details that were not observed with the previously used electrode grids. For example, the findings that the cardiac impulse can originate from extranodal sites within the right atrium [35] or that reentrant wavefronts in the human heart are highly organized [36].

To date optical mapping is the method of choice for determining activation and repolarization patterns in transgenic mice [37–41]. It is frequently used for mapping cardiac tissue preparations of larger mammals including man [42–44]. It is also applied to measure monolayers that are nowadays often used to test gene therapy [45] or to characterize cardiomyocytes derived from induced pluripotent stem (iPS) cells from human [46]. However, as with single cell experiments, phototoxicity is a limitation of optical mapping when imaging monolayers [29].

## B. Panoramic imaging

Despite the superior high spatial resolution of optical mapping, the activation front propagates outside the two-dimensional field of view, especially during ventricular fibrillation. In 1999, this problem was addressed by measuring the opposite side of the heart using mirrors [47]. Later, panoramic imaging was performed with multiple cameras [48]. Panoramic imaging allowed to measure the complete epicardial activation sequences during ventricular fibrillation (Fig 5) [49, 50]. In conventional optical mapping, a curved epicardial surface is projected onto a 2-dimensional sensor. This means that distance in the “Z” direction is not taken into account when conduction velocity is calculated and may lead to underestimation of conduction velocity, especially near the edges of the field of view. Panoramic imaging enables the projection of a 3-dimensional conduction pattern on the surface of the heart. Conduction velocity can be more precisely measured thereby improving our understanding of conduction during normal and irregular activation patterns [51]. Despite these advances, panoramic imaging is still limited to the surface of the heart and cannot measure three-dimensional pattern of excitation across the transmural myocardium.

## C. Transmural imaging: transillumination

Conventional optical mapping records sub-surface epicardial or endocardial activation patterns. However, the transmural activation pattern is critically important in the mechanism of arrhythmias. Local electrograms recorded with plunge needle electrodes provide information about the moment of activation and repolarization but with low spatial

resolution [52, 53]. An optical method was proposed to address the issue of transmural activation and repolarization [54]. Zemlin et al showed that the morphology of the upstroke reveals the direction of propagation of the 3-dimensional wavefront near the surface [55]. Application of near infrared dyes also allowed pseudo-three-dimensional imaging by using transillumination techniques [56, 57]. However, a more rigorous inverse problem solution would be required to address three-dimensional pattern of activation.

## V. Optics for monitoring intra cellular ion concentration

### A. Calcium imaging

Depolarization of the cardiac cell membrane results in an influx of  $\text{Ca}^{2+}$  that triggers the sarcoplasmic reticulum to release its stored  $\text{Ca}^{2+}$  causing a rise in the cytoplasmic  $\text{Ca}^{2+}$  and contraction of the cardiomyocyte [58]. This mechanism, referred to as excitation-contraction-coupling, is the link between electrical activation and contraction, therefore it is important to be able to monitor it. Several fluorescent dyes have been found to change their emission spectrum or fluorescence upon binding  $\text{Ca}^{2+}$  (expertly reviewed in [59]). It is important to realize that with this technique the amount of  $\text{Ca}^{2+}$  that is bound to the dye is measured and not the free  $\text{Ca}^{2+}$  concentration. Another important related consideration is how to strike a right balance between signal quality and calcium buffering. High affinity calcium dyes yield better signal-to-noise ratio, but alter calcium handling by buffering free calcium leading to an error in the measured calcium concentration; in contrast, low affinity dyes do not interfere with physiological calcium cycling, but are notoriously difficult to use due to low quality of signals [60–62]. In 1967, the first fluorescence-based measurement of  $\text{Ca}^{2+}$  was performed using aquarin [63]. After that, other indicators were discovered such as Indo-1, Fluo-3/4, Fura-2 and Rhod-2 [64–68]. Free intra-cellular  $\text{Ca}^{2+}$  was first measured by fluorescence in the beating heart in the late 1980s using  $\text{Ca}^{2+}$  indicator Indo-1 [69]. The introduction of laser scanning and multiphoton microscopy has enabled the discovery of  $\text{Ca}^{2+}$  subcellular localization and the detection of  $\text{Ca}^{2+}$  sparks (reviewed in [70]).

### B. Sodium and potassium imaging

The intra and extra cellular concentrations of  $\text{Na}^+$  and  $\text{K}^+$  are major determinants of conduction and repolarization in the myocardium. Fluorescent indicators of  $\text{Na}^+$  and  $\text{K}^+$  used in cardiac research, SBFI and PBFI respectively were discovered in the late 1980s [71, 72]. The use of SBFI enabled easy detection of intracellular  $\text{Na}^+$  concentration during heart failure [73]. PBFI has been used to monitor  $\text{K}^+$  concentration during hypoxia [74]. Most of the experiments are done in isolated cardiomyocytes. To our knowledge, in the intact heart, no studies have been done in which  $\text{Na}^+$  and  $\text{K}^+$  are measured using fluorescent indicators. However, changes in extracellular  $\text{K}^+$  throughout the myocardium have been directly related to heterogeneity in refractoriness and the onset of arrhythmias [75]. Therefore, we think that the application of high resolution optical mapping of  $\text{Na}^+$  and  $\text{K}^+$  in the intact heart could advance our knowledge about the mechanisms of ischemia induced or triggered arrhythmias.

### C. Metabolic imaging

During ischemia or heart failure many changes occur in the mitochondria, in particular changes in the inner membrane potential, which is of critical importance [76]. The

membrane potential of mitochondria can be monitored using fluorescent indicators, such as Safranin [77] or more recently developed dyes such as JC-1, Rhodamine 123 and its derivatives TMRE and TMRM [78–81]. These dyes have primarily been used in isolated mitochondrial and cellular studies, but recently have been administered in isolated hearts. In the later it appeared that brief periods of ischemia induced a collapse of the mitochondrial membrane potential that spreads as a propagating wave across the myocardium [82]. Although the use of mitochondrial membrane potential dye in the whole heart is debated [83], this is potentially a powerful method that would allow mechanistic insight into the relation between cardiac metabolic state and its excitation-contraction coupling.

The metabolic state is also reflected by the levels of NADH [84], which bears its own intrinsic fluorescence properties. The reduction of NAD<sup>+</sup> to NADH represents a decreased ability to generate ATP and results in an increase in fluorescence (excitation: 366±15 nm, emission: 485±15 nm). Although its spectrum may interfere with optical measurements of other intracellular ion concentration [85] it allows to relate NADH levels to cardiac electrophysiology without the need for extrinsic fluorophore [86]. The same accounts for the intrinsic absorption changes of mitochondrial cytochromes or the transition of oxy into deoxy hemoglobin and myoglobin [87]. Another important parameter in the metabolic state is the pH, which can be measured with the fluorescent indicator SNARF-1 [88]. The metabolic state of the myocardium may precede and cause electrophysiological changes and predict when and where in the heart arrhythmias will occur.

#### D. Multiparametric imaging

The development of fluorescent dyes for ions and or metabolic parameters made it easy to monitor differences in ion concentration during the action potential (Fig 6). The first measurement of membrane potential and intracellular calcium in the same heart co-loaded with both voltage- and calcium-sensitive dyes were done in 1994 [89] and became common in the early 2000s [60, 90–92]. This confirmed the previously suggested relation between spontaneous calcium releases and delayed afterdepolarization (DAD) as mechanism underlying triggered activity in heart failure (Fig 6) [93, 94]. The combination of dyes, however, should be chosen with care. The combination of RH-237/Rhod-2 or di-4-ANEPPS/Indo-1, allows to record simultaneously whereas the use of Fluo-3/4/di-4-ANEPPS results in an error because of the overlap in emission spectrum of the two dyes [90, 92–94].

## VI. Technology development

### A. Photodetectors

In the begin 1970s photomultipliers were used to measure the change in fluorescence of single cells [16]. Although photomultipliers lack the ability to store spatial information they have a high photosensitivity and allow sampling up to 100 kHz. To date, photomultipliers are still used for single cell experiments [95]. Multi anode photomultipliers have a low spatial resolution and are not suitable for mapping experiments. Therefore, in the early 1980s laser scanning was combined with photomultipliers to detect propagation of the activation front in the heart [96]. However, the spatial resolution was hampered by sequential recordings and, therefore, failed to resolve a single activation front. The first

camera that provided a spatial resolution that was comparable to conventional multi-electrode grids used photodiode arrays for detection of fluorescence (12×12 or 16×16 pixels). The chip of a diode array is made of individual diodes with a large dimension allowing to measure at low light intensities. Also, the ability to control the feedback resistor of current-to-voltage converters, which increases the dynamic range, allows to image small fractional changes of fluorescence at high background levels [97]. The charge-coupled device (CCD) cameras were the first that provided a spatial resolution that was higher than what could be achieved when using conventional multielectrode grids (128×128 pixels). The increase in spatial resolution, however, reduces the maximum sampling frequency (+/- 500 frames per second) and the dynamic range ( $10^3$ ), even in the newer developed electron multiplying CCD cameras [6, 98]. This is a major disadvantage because signal to noise ratio is positively related to the light intensity. Alternative imaging technology, which became dominant due to superior signal-to-noise ratio, is based on complementary metal oxide semiconductor (CMOS) technology. It has a high spatial resolution of 100×100 pixels, a high signal-to-noise ratio and can sample up 10,000 frames per second. Also the dynamic range is comparable with that of the diode array (CMOS: $10^5$  vs diode array:  $10^6$ ) [97].

The existing fast CMOS system is expensive due to the requirement of a sub-system for the acquisition of optical signals, which has to be developed by the industry. However, a recent advancement in technology may offer a long-awaited solution to the cost problem. Several imaging companies developed fast CMOS and CCD cameras with a standard USB-3 interface, which allows sufficient sampling rate without compromising spatial resolution. The cost of USB-3 based imaging system reduces the cost for an optical set-up from over a hundred thousand dollars to fewer than ten thousand dollars [99]. Furthermore, an USB-3 based system enables scaling down the size of the setup, which not achievable with the previous mentioned systems. An imaging system with up to ten CMOS USB-3 cameras could be built at a cost of ~\$10,000–\$15,000.

## B. Light Sources

The intensity and homogeneity of excitation light is of crucial importance for the quality of optical signals. The first optical experiments were performed using halogen lamps [17] and are still used today [21, 25]. Other sources used in optocardiography are based on arc using mercury and/or xenon [60]. Both arc and halogen lamps require filters in order to provide light of the requested excitation wavelength. Although these light sources provide sufficient excitation light intensity, there is room for improvement. Arc lamps are unstable because of plasma oscillations and thermal runaway. Furthermore, for the stable excitation light a highly regulated voltage supply is required which makes arc and halogen based light sources relative expensive. Light Emitting Diodes (LEDs) have recently emerged as a qualitatively better and cheaper alternative for the traditional light sources [100–102]. LEDs exist with one specific wavelength, which make excitation filters superfluous when only one fluorophore is used. Furthermore, LEDs can be turned off and on within the order of microseconds which makes them ideal for dual wavelength excitation. The small size of LEDs allows the building of a multi-LED light source that provides enough light for measurements of the intact heart or small tissue preparations [38, 103]. A disadvantage of the use of LEDs is that cooling is required and, furthermore, there is non-linear relation

between input current and light output. However, these matters can easily be addressed which makes LEDs the preferable light source for optical experiments.

### C. Calibration and Motion artifacts

While interpreting optical data it is important to remember that optical signals are measured as arbitrary units and do not represent absolute voltage or concentration. Furthermore, contraction of the heart can result in a change in fluorescence independent of change in voltage or concentration. These changes are called motion artifacts. One method to address both calibration and motion artifact issues is based on so called ratiometric measuring. The use of optical indicators with multiple excitation and emission spectra enables ratiometric measuring and elimination of subtle motion artifacts. For  $\text{Ca}^{2+}$  measurements the fluorescent dyes Indo-1 or Fura-2 (Reviewed in [59]) can be used whereas for voltage measuring the recently developed Pittsburgh dyes are suitable [23].

To eliminate motion in the X and Y direction contraction needs to be uncoupled from electrical activation. Several pharmacologic agents have been used to reduce motion [104–106]. A common used agent is 2,3-butanedione monoxime (BDM). Although the use of BDM reduces motion it has a major effect on calcium handling, conduction and repolarization [107, 108]. The recently discovered myosin II inhibitor blebbistatin [109] is, therefore, a preferable candidate for reduction of motion artifacts [106, 110]. The use of blebbistatin has recently been debated [111] but has been shown to have no effect on cardiac electrophysiology [106, 110]. However, blebbistatin may improve cardiac function during metabolic stress due to inhibition of the major ATP consumer  $\text{Mg}^{2+}$  ATP-ase, responsible for mechanical contraction.

### D. Signal processing

Optical signals arise from a spectral shift of the emission light from the fluorescent dye after a change in membrane potential or binding an ion. The fractional change of fluorescence is small (1%–12%). The need for a high acquisition rate results in optical signals with a low signal-to-noise ratio [112]. For that reason, spatial binning of pixels or temporal filtering is often required to generate signals that are suitable for analysis (reviewed in [113]). However, binning of pixels reduces spatial resolution and filter settings can alter morphology of signals in such a way that it does not represent the physiological processes from the area where it was recorded [113, 114]. Although optical mapping is accepted technique for monitoring cardiac electrophysiology, there is a shortage of standards for signal and image analysis. Our laboratory has developed an open-source MATLAB-based analysis software for optical signals which is freely available at <http://code.google.com/p/rhythm-analysis-software/> [113].

## VII. Optically measuring cardiac mechanics

Recently, structured light imaging has been used to monitor cardiac mechanics [115]. Structured light imaging uses the deformation of projected light to reconstruct a 3-dimensional surface. The advantage of this technique compared to others, like MRI or video-based techniques, is that it has a high resolution (10–100 micrometer) [116–119]. The



combination of structural light imaging with optical mapping [120] could be used to study the dissociation between contraction and membrane potentials during ventricular fibrillation or global ischemia [121]. Structured light could also become the basis for correcting optical signals for motion artifacts. Until now, monitoring of two-dimensional motion has been used to correct optical action potentials [122, 123]. However, for sufficient correction, motion and electrophysiology should be measured with a similar resolution. Although optimization is required, we think that in the future structured light could be used for eliminating motion artifacts in optical signals. In this way the use of pharmacological excitation-contraction uncouplers has become unnecessary and optical experiments become more physiological.

## VIII. Optogenetics: control of cardiac function

In 2006 a new field emerged and was named “optogenetics” [124]. As the name suggests, it combines optic and genetic approaches to interfere with physiology. As for conventional optical mapping optogenetics finds its roots in the field of neurology [125]. Optogenetics is based on ectopic expression of light-gated ion channels of which channelrhodopsin1 and channelrhodopsin2 are the first to be used [126, 127]. Light-gated ion channels can generate a “photocurrent” that is sufficient for stimulating or controlling neurons [128].

Optogenetics has been introduced to cardiac electrophysiology only recently (extensively reviewed in [8]). It has been shown that in the intact heart optogenetics can be used to silence spontaneous active cardiomyocytes and activate quiescent cardiomyocytes [7, 129, 130]. The possibility to express channelrhodopsin only in specific cell types [131] will allow stimulation or inhibition of cell types in the heart like neurons or Purkinje cells. The latter was not possible with the same precision using conventional (micro) electrodes. Thus, optogenetics provide important new tools for studying the role of the nervous system in atrial fibrillation or the role Purkinje fibers in (ischemia-induced) ventricular fibrillation. In addition, specific overexpression using a lenti-virus [132] may enable a future for channelrhodopsin in clinical cardiology. Taken together, we think that the use optogenetics will lead to important new discoveries in cardiac physiology.

## IX. The Optrode: transmural optical recordings

The idea of using an optical fiber to carry both the excitation and emission light was first conceived by Neunlist et al, who coined the term “optrode” in 1992 [133]. In 2001, Hooks and colleagues developed a novel optical system that enabled transmural recording of transmembrane potentials using a bundled “optrode” approach (Fig 7) [134]. Transmural activation patterns are involved in the genesis of the QRS complex but also in arrhythmogenesis [52, 135]. Thus, the invention of the optrode was an important contribution to the field of the optical mapping that until then was restricted to measurements only from the surface of the endocardium or epicardium. Further development of the optrode resulted to better signals and clear transmural recordings of optical action potentials [136, 137]. We think that the use of the optrode will contribute to the ongoing debate about the origin of the T-wave [138, 139]. Furthermore, in patients with atrial fibrillation, the area where complex fractionated atrial electrograms (CFAEs) are measured is ablated [140]. The mechanisms of these CFAEs are diverse and not completely

understood [141]. We think that the recording of optical action potential with the optrode will contribute to understanding these CFAEs and the mechanism of atrial fibrillation. Another important application of the transmural optrode approach is dual imaging of action potentials and calcium transients. Recently, it demonstrated dramatic uncoupling between excitation and contraction due to altered calcium handling during unsupported ventricular fibrillation [121].

## X. Limitation of Optocardiography

To date, the use of optocardiographic methods are well accepted in basic cardiac research. However, as briefly mentioned above, there are also limitations of optical methods. A disadvantage of the use of potentiometric dyes is that only the relative change in potential is measured and not the absolute potentials. In addition, potentiometric dyes have been reported to exhibit phototoxicity in isolated cells and cell culture preparations [28]. Furthermore, heterogeneous loading and/or excitation may lead to different signal-to-noise ratios throughout the tissue preparation and may influence signal processing and interpretation. It has also been suggested that the use of di-4-ANEPPS and excitation contraction uncoupler blebbistatin may alter cardiac electrophysiology [111, 142]. The same is true for high affinity fluorescent calcium indicators that can buffer free calcium and thereby alter calcium handling [59]. These matters should be taken into account when the choice is made to use optical measuring methods.

In clinical cardiology optical mapping methods are not used to monitor electrophysiology. The main reason for that is that potentiometric dyes are required for measuring optical action potentials. The *in vivo* effects of these dyes in human physiology are not well investigated and, therefore, are not (yet) allowed. Another disadvantage is that commonly used CCD or CMOS based camera systems have a bottleneck in slow image visualization which, therefore, limits their use for real time monitoring of optical action potentials. In contrast, photodiode arrays do have the capability to measure and visualize real-time. However, it comes at the cost of the spatial resolution, which does not exceed that of conventional multi-electrode grids. New USB-3 CMOS cameras are likely to address this problem by providing relatively inexpensive imaging systems.

## XI. Conclusion and future perspectives

The first electrical and optical experiments in the field of cardiology were performed around the end of XIX century. After that, electrocardiography developed into the dominant method for recording and intervention in experimental and clinical cardiology. However, optocardiography has made a fast progression in the last 3 decades and now exceeds electrocardiography in way that it allows stimulation and recording with a higher spatial resolution. Therefore, in the experimental setting, roughly all electrophysiological experiments are done optically. Furthermore, optocardiography has the advantage of multiparametric imaging enabling multi-integrative cardiac physiology. The latter is not possible with electrocardiographic methods and will help unraveling the relation between cardiac metabolism and electrophysiology. In the clinic, however, electrocardiographic methods are still superior for recording and stimulation. Nevertheless, we speculate that the

development of an advanced optrode will introduce optocardiography to the clinic. The ability to apply high-resolution optical mapping in-vivo enables the detection of micro re-entry circuits or ectopic foci and which will contribute to the treatment of patients with arrhythmias.

## Acknowledgments

This work was supported by NIH grants R21-HL112278, R01-HL114395, and R01-HL115415.

## References

1. Waller AD. A Demonstration on Man of Electromotive Changes accompanying the Heart's Beat. *J Physiol.* Oct.1887 8:229–34.
2. Koelliker RAMH. Nachweis der negativen Schwankung des Muskelstroms am natürlich sich contrahirenden Muskel. *Verhandlungen der Physikalisch-medizinische Gesellschaft in Würzburg.* 1856; 6:15.
3. Oster HS, Taccardi B, Lux RL, Ershler PR, Rudy Y. Noninvasive electrocardiographic imaging: reconstruction of epicardial potentials, electrograms, and isochrones and localization of single and multiple electrocardiac events. *Circulation.* Aug 5.1997 96:1012–24. [PubMed: 9264513]
4. Lewalter, TLB. Historical Milestones of Electrical Signal Recording and Analysis. In: Gussak, IAC., editor. *Briding Basic and Clinical Science.* New Jersey: Humana Press Inc; 2010. p. 7-21.
5. Efimov IR, Nikolski VP, Salama G. Optical imaging of the heart. *Circulation Research.* 2004; 95:21–33. [PubMed: 15242982]
6. Herron TJ, Lee P, Jalife J. Optical imaging of voltage and calcium in cardiac cells & tissues. *Circ Res.* Feb 17.2012 110:609–23. [PubMed: 22343556]
7. Bruegmann T, Malan D, Hesse M, Beiert T, Fuegemann CJ, Fleischmann BK, et al. Optogenetic control of heart muscle in vitro and in vivo. *Nat Methods.* Nov.2010 7:897–900. [PubMed: 20881965]
8. Entcheva E. Cardiac optogenetics. *Am J Physiol Heart Circ Physiol.* May.2013 304:H1179–91. [PubMed: 23457014]
9. Marey EJLG. Inscription photographique des indications des l'ectromètre de Lippmann. *C R Acad Sci.* 1876; 83:2.
10. Bull L. Motional mechanism of the insect wing. *Comptes Rendus de l'Académie des Sciences.* 1904; 138:2.
11. Mines GR. On functional analysis by the action of electrolytes. *J Physiol.* Jun 19.1913 46:188–235. [PubMed: 16993198]
12. Wiggers CJ. The Mechanism and Nature of Ventricular Fibrillation. *Am Heart J.* 1940; 20:399–412.
13. Wiggers CJ, Bell JR, Paine M. Studies of ventricular fibrillation caused by electric shock: II. Cinematographic and electrocardiographic observations of the natural process in the dog's heart. Its inhibition by potassium and the revival of coordinated beats by calcium. *Ann Noninvasive Electrocardiol.* Jul.2003 8:252–61. discussion 251. [PubMed: 14510663]
14. Cohen LB, Keynes RD, Hille B. Light scattering and birefringence changes during nerve activity. *Nature.* 1968; 218:438–441. [PubMed: 5649693]
15. Cohen LB, Salzberg BM. Optical measurement of membrane potential. *Rev Physiol Biochem Pharmacol.* 1978; 83:35–88. [PubMed: 360357]
16. Salzberg BM, Davila HV, Cohen LB. Optical recording of impulses in individual neurones of an invertebrate central nervous system. *Nature.* 1973; 246:508–9. [PubMed: 4357630]
17. Salama G, Morad M. Merocyanine 540 as an optical probe of transmembrane electrical activity in the heart. *Science.* Feb 6.1976 191:485–487. [PubMed: 1082169]
18. Ross WN, Salzberg BM, Cohen LB, Davila HV. A large change in dye absorption during the action potential. *Biophys J.* 1974; 14:983–6. [PubMed: 4429774]

19. Davila HV, Salzberg BM, Cohen LB, Waggoner AS. A large change in axon fluorescence that provides a promising method for measuring membrane potential. *Nat New Biol.* 1973; 241:159–60. [PubMed: 4512623]
20. Loew LM, Benson L, Lazarovici P, Rosenberg I. Fluorometric analysis of transferable membrane pores. *Biochemistry.* Apr 23.1985 24:2101–2104. [PubMed: 2581609]
21. Efimov IR, Huang DT, Rendt JM, Salama G. Optical mapping of repolarization and refractoriness from intact hearts. *Circulation.* Sep.1994 90:1469–1480. [PubMed: 8087954]
22. Windisch H, Muller W, Tritthart HA. Fluorescence monitoring of rapid changes in membrane potential in heart muscle. *Biophysical Journal.* Dec.1985 48:877–884. [PubMed: 2418888]
23. Salama G, Choi BR, Azour G, Lavasani M, Tumbev V, Salzberg BM, et al. Properties of new, long-wavelength, voltage-sensitive dyes in the heart. *J Membr Biol.* Nov.2005 208:125–40. [PubMed: 16645742]
24. Matiukas A, Mitrea BG, Pertsov AM, Wuskell JP, Wei MD, Watras J, et al. New near-infrared optical probes of cardiac electrical activity. *Am J Physiol Heart Circ Physiol.* Jun.2006 290:H2633–43. [PubMed: 16399869]
25. Matiukas A, Mitrea BG, Qin M, Pertsov AM, Shvedko AG, Warren MD, et al. Near-infrared voltage-sensitive fluorescent dyes optimized for optical mapping in blood-perfused myocardium. *Heart Rhythm.* Nov.2007 4:1441–51. [PubMed: 17954405]
26. Muller W, Windisch H, Tritthart HA. Fluorescent styryl dyes applied as fast optical probes of cardiac action potential. *Eur Biophys J.* 1986; 14:103–111. [PubMed: 3816701]
27. Fedorov VV, Schuessler RB, Hemphill M, Ambrosi CM, Chang R, Voloshina AS, et al. Structural and Functional Evidence for Discrete Exit Pathways That Connect the Canine Sinoatrial Node and Atria. *Circ Res.* Feb 26.2009
28. Schaffer P, Ahammer H, Muller W, Koidl B, Windisch H. Di-4-ANEPPS causes photodynamic damage to isolated cardiomyocytes. *Pflugers Arch.* Apr.1994 426:548–551. [PubMed: 8052525]
29. Fast VG, Kleber AG. Anisotropic conduction in monolayers of neonatal rat heart cells cultured on collagen substrate. *Circulation Research.* Sep.1994 75:591–595. [PubMed: 8062430]
30. Efimov IR, Fahy GJ, Cheng YN, Van Wagoner DR, Tchou PJ, Mazgalev TN. High Resolution Fluorescent Imaging of Rabbit Heart Does Not Reveal A Distinct Atrioventricular Nodal Anterior Input Channel (Fast Pathway) During Sinus Rhythm. *Journal of Cardiovascular Electrophysiology.* 1997; 8:295–306. [PubMed: 9083879]
31. Kamino K, Hirota A, Fujii S. Localization of pacemaking activity in early embryonic heart monitored using voltage-sensitive dye. *Nature.* Apr 16.1981 290:595–597. [PubMed: 7219544]
32. Efimov IR, Aguel F, Cheng Y, Wollenzier B, Trayanova N. Virtual Electrode Polarization in the Far Field: Implications for External Defibrillation. *Am J Physiol.* 2000; 279:H1055–H1070.
33. Muller W, Windisch H, Tritthart HA. Fast optical monitoring of microscopic excitation patterns in cardiac muscle. *Biophysical Journal.* Sep.1989 56:623–629. [PubMed: 2790142]
34. Rosenbaum, DS.; Jalife, J. *Optical mapping of cardiac excitation and arrhythmias.* Armonk, NY: Futura Publishing; 2002.
35. Bromberg BI, Hand DE, Schuessler RB, Boineau JP. Primary negativity does not predict dominant pacemaker location: implications for sinoatrial conduction. *Am J Physiol.* 1995; 269:H877–H887. [PubMed: 7573531]
36. Nanthakumar K, Jalife J, Masse S, Downar E, Pop M, Asta J, et al. Optical mapping of Langendorff-perfused human hearts: establishing a model for the study of ventricular fibrillation in humans. *Am J Physiol Heart Circ Physiol.* Jul.2007 293:H875–80. [PubMed: 17369453]
37. Bezzina CR, Barc J, Mizusawa Y, Remme CA, Gourraud JB, Simonet F, et al. Common variants at SCN5A-SCN10A and HEY2 are associated with Brugada syndrome, a rare disease with high risk of sudden cardiac death. *Nat Genet.* Jul 21.2013
38. Boukens BJ, Sylva M, de Gier-de Vries C, Remme CA, Bezzina CR, Christoffels VM, et al. Reduced sodium channel function unmasks residual embryonic slow conduction in the adult right ventricular outflow tract. *Circ Res.* Jul 5.2013 113:137–41. [PubMed: 23661717]
39. Nygren A, Clark RB, Belke DD, Kondo C, Giles WR, Witkowski FX. Voltage-sensitive dye mapping of activation and conduction in adult mouse hearts. *Annals of Biomedical Engineering.* 2000; 28:958–967. [PubMed: 11144681]

40. Rentschler S, Harris BS, Kuznekoff L, Jain R, Manderfield L, Lu MM, et al. Notch signaling regulates murine atrioventricular conduction and the formation of accessory pathways. *J Clin Invest.* 2011; 121:525–533. [PubMed: 21266778]
41. Boukens BJ, Hoogendijk MG, Verkerk AO, Linnenbank A, van Dam P, Remme CA, et al. Early repolarization in mice causes overestimation of ventricular activation time by the QRS duration. *Cardiovasc Res.* Jan 1.2013 97:182–91. [PubMed: 22997159]
42. Glukhov AV, Fedorov VV, Lou Q, Ravikumar VK, Kalish PW, Schuessler RB, et al. Transmural Dispersion of Repolarization in Failing and Nonfailing Human Ventricle. *Circ Res.* Jan 21.2010 106:981–91. [PubMed: 20093630]
43. Fedorov VV, Glukhov AV, Chang R, Kostecki G, Aferol H, Hucker WJ, et al. Optical mapping of the isolated coronary-perfused human sinus node. *J Am Coll Cardiol.* 2010 vol. in press.
44. Greener ID, Monfredi O, Inada S, Chandler NJ, Tellez JO, Atkinson A, et al. Molecular architecture of the human specialised atrioventricular conduction axis. *Journal of molecular and cellular cardiology.* Apr.2011 50:642–51. [PubMed: 21256850]
45. Bakker ML, Boink GJ, Boukens BJ, Verkerk AO, van den Boogaard M, den Haan AD, et al. T-box transcription factor TBX3 reprogrammes mature cardiac myocytes into pacemaker-like cells. *Cardiovasc Res.* Jun 1.2012 94:439–49. [PubMed: 22419669]
46. Lee P, Klos M, Bollensdorff C, Hou L, Ewart P, Kamp TJ, et al. Simultaneous voltage and calcium mapping of genetically purified human induced pluripotent stem cell-derived cardiac myocyte monolayers. *Circ Res.* Jun 8.2012 110:1556–63. [PubMed: 22570367]
47. Lin SF, Wikswo JP. Panoramic optical imaging of electrical propagation in isolated heart. *Journal of Biomedical Optics.* Apr.1999 4:200–207. [PubMed: 23015205]
48. Kay MW, Amison PM, Rogers JM. Three-dimensional surface reconstruction and panoramic optical mapping of large hearts. *IEEE Trans Biomed Eng.* 2004; 51:1219–1229. [PubMed: 15248538]
49. Qu F, Ripplinger CM, Nikolski VP, Grimm C, Efimov IR. Three-dimensional panoramic imaging of cardiac arrhythmias in rabbit heart. *J Biomed Opt.* Jul-Aug;2007 12:044019. [PubMed: 17867823]
50. Rogers JM, Walcott GP, Gladden JD, Melnick SB, Kay MW. Panoramic optical mapping reveals continuations epicardial reentry during ventricular fibrillation in the isolated swine heart. *Biophys.* 2007; 92:1090–1095.
51. Lou Q, Ripplinger CM, Bayly PV, Efimov IR. Quantitative panoramic imaging of epicardial electrical activity. *Ann Biomed Eng.* Oct.2008 36:1649–58. [PubMed: 18654852]
52. Durrer D, Dam RTv, Freud GE, Janse MJ, Meijler FL, Arzbacher RC. Total excitation of the isolated human heart. *Circulation.* Jun.1970 41:899–912. [PubMed: 5482907]
53. Ophhof T, Coronel R, Wilms-Schopman FJ, Plotnikov AN, Shlapakova IN, Danilo P Jr, et al. Dispersion of repolarization in canine ventricle and the electrocardiographic T wave: Tp-e interval does not reflect transmural dispersion. *Heart Rhythm.* Mar.2007 4:341–8. [PubMed: 17341400]
54. Bernus O, Wellner M, Mironov SF, Pertsov AM. Simulation of voltage-sensitive optical signals in three-dimensional slabs of cardiac tissue: application to transillumination and coaxial imaging methods. *Phys Med Biol.* Jan 21.2005 50:215–29. [PubMed: 15742940]
55. Zemlin CW, Bernus O, Matiukas A, Hyatt CJ, Pertsov AM. Extracting intramural wavefront orientation from optical upstroke shapes in whole hearts. *Biophys J.* Jul.2008 95:942–50. [PubMed: 18390615]
56. Bernus O, Mukund KS, Pertsov AM. Detection of intramyocardial scroll waves using absorptive transillumination imaging. *J Biomed Opt.* Jan-Feb;2007 12:014035. [PubMed: 17343510]
57. Walton RD, Xavier CD, Tachtsidis I, Bernus O. Experimental validation of alternating transillumination for imaging intramural wave propagation. *Conf Proc IEEE Eng Med Biol Soc.* 2011; 2011:1676–9. [PubMed: 22254647]
58. Bers DM. Cardiac excitation-contraction coupling. *Nature.* Jan 10.2002 415:198–205. [PubMed: 11805843]
59. Takahashi A, Camacho P, Lechleiter JD, Herman B. Measurement of intracellular calcium. *Physiol Rev.* Oct.1999 79:1089–125. [PubMed: 10508230]

60. Fast VG. Simultaneous optical imaging of membrane potential and intracellular calcium. *J Electrocardiol.* Oct.2005 38:107–12. [PubMed: 16226084]
61. Fast VG, Ideker RE. Simultaneous optical mapping of transmembrane potential and intracellular calcium in myocyte cultures. *J Cardiovasc Electrophysiol.* 2000; 11:547–556. [PubMed: 10826934]
62. Escobar AL, Monck JR, Fernandez JM, Vergara JL. Localization of the site of Ca<sup>2+</sup> release at the level of a single sarcomere in skeletal muscle fibres. *Nature.* Feb 24.1994 367:739–41. [PubMed: 8107869]
63. Ridgway EB, Ashley CC. Calcium transients in single muscle fibers. *Biochem Biophys Res Commun.* Oct 26.1967 29:229–34. [PubMed: 4383681]
64. Kihara Y, Grossman W, Morgan JP. Direct measurement of changes in intracellular calcium transients during hypoxia, ischemia, and reperfusion of the intact mammalian heart. *Circulation Research.* 1989; 65:1029–1044. [PubMed: 2791218]
65. Knisley, SB. Mapping intracellular calcium in rabbit hearts with fluo 3. *Proc 17th Annu Int Conf IEEE Eng Med Biol Soc ed;* 1995. p. 455-456.
66. del Nido PJ, Glynn P, Buenaventura P, Salama G, Koretsky AP. Fluorescence measurement of calcium transients in perfused rabbit heart using rhod 2. *Am J Physiol.* 1998; 274:H728–H741. [PubMed: 9486280]
67. MacGowan GA, Du C, Glonty V, Suhan JP, Koretsky AP, Farkas DL. Rhod-2 based measurements of intracellular calcium in the perfused mouse heart: cellular and subcellular localization and response to positive inotropy. *J Biomed Opt.* 2001; 6:23–30. [PubMed: 11178577]
68. Minta A, Kao JP, Tsien RY. Fluorescent indicators for cytosolic calcium based on rhodamine and fluorescein chromophores. *J Biol Chem.* May 15.1989 264:8171–8. [PubMed: 2498308]
69. Lee KS. Potentiation of the calcium-channel currents of internally perfused mammalian heart cells by repetitive depolarization. *Proc Natl Acad Sci U S A.* Jun.1987 84:3941–5. [PubMed: 2438689]
70. Rubart M. Two-photon microscopy of cells and tissue. *Circ Res.* Dec 10.2004 95:1154–66. [PubMed: 15591237]
71. Jezek P, Mahdi F, Garlid KD. Reconstitution of the beef heart and rat liver mitochondrial K<sup>+</sup>/H<sup>+</sup> (Na<sup>+</sup>/H<sup>+</sup>) antiporter. Quantitation of K<sup>+</sup> transport with the novel fluorescent probe, PBFI. *J Biol Chem.* Jun 25.1990 265:10522–6. [PubMed: 2162352]
72. Minta A, Tsien RY. Fluorescent indicators for cytosolic sodium. *J Biol Chem.* Nov 15.1989 264:19449–57. [PubMed: 2808435]
73. Baartscheer A, Schumacher CA, Belterman CN, Coronel R, Fiolet JW. [Na<sup>+</sup>]<sub>i</sub> and the driving force of the Na<sup>+</sup>/Ca<sup>2+</sup>-exchanger in heart failure. *Cardiovasc Res.* Mar 15.2003 57:986–95. [PubMed: 12650876]
74. Shieh RC, Goldhaber JI, Stuart JS, Weiss JN. Lactate transport in mammalian ventricle. General properties and relation to K<sup>+</sup> fluxes. *Circ Res.* May.1994 74:829–38. [PubMed: 8156630]
75. Coronel R, Fiolet JW, Wilms-Schopman FJ, Schaapherder AF, Johnson TA, Gettes LS, et al. Distribution of extracellular potassium and its relation to electrophysiologic changes during acute myocardial ischemia in the isolated perfused porcine heart. *Circulation.* May.1988 77:1125–1138. [PubMed: 3359590]
76. Chen LB. Mitochondrial membrane potential in living cells. *Annu Rev Cell Biol.* 1988; 4:155–81. [PubMed: 3058159]
77. Akerman KE, Wikstrom MK. Safranin as a probe of the mitochondrial membrane potential. *FEBS Lett.* Oct 1.1976 68:191–7. [PubMed: 976474]
78. Smith JC. Potential-sensitive molecular probes in membranes of bioenergetic relevance. *Biochim Biophys Acta.* Mar 15.1990 1016:1–28. [PubMed: 2178682]
79. Emaus RK, Grunwald R, Lemasters JJ. Rhodamine 123 as a probe of transmembrane potential in isolated rat-liver mitochondria: spectral and metabolic properties. *Biochim Biophys Acta.* Jul 23.1986 850:436–48. [PubMed: 2873836]
80. Matsumoto-Ida M, Akao M, Takeda T, Kato M, Kita T. Real-time 2-photon imaging of mitochondrial function in perfused rat hearts subjected to ischemia/reperfusion. *Circulation.* Oct 3.2006 114:1497–503. [PubMed: 17000908]

81. Smiley ST, Reers M, Mottola-Hartshorn C, Lin M, Chen A, Smith TW, et al. Intracellular heterogeneity in mitochondrial membrane potentials revealed by a J-aggregate-forming lipophilic cation JC-1. *Proc Natl Acad Sci U S A*. May 1.1991 88:3671–5. [PubMed: 2023917]
82. Lyon AR, Joudrey PJ, Jin D, Nass RD, Aon MA, O'Rourke B, et al. Optical imaging of mitochondrial function uncovers actively propagating waves of mitochondrial membrane potential collapse across intact heart. *J Mol Cell Cardiol*. Oct.2010 49:565–75. [PubMed: 20624394]
83. Scaduto RC Jr, Grottyohann LW. Measurement of mitochondrial membrane potential using fluorescent rhodamine derivatives. *Biophys J*. Jan.1999 76:469–77. [PubMed: 9876159]
84. Chance B, Salkovitz IA, Kovach AG. Kinetics of mitochondrial flavoprotein and pyridine nucleotide in perfused heart. *Am J Physiol*. 1972; 223:207–218. [PubMed: 4339003]
85. Donoso P, Mill JG, O'Neill SC, Eisner DA. Fluorescence measurements of cytoplasmic and mitochondrial sodium concentration in rat ventricular myocytes. *J Physiol*. Mar.1992 448:493–509. [PubMed: 1593474]
86. Salama G, Lombardi R, Elson J. Maps of optical action potentials and NADH fluorescence in intact working hearts. *American Journal of Physiology*. Feb.1987 252:H384–94. [PubMed: 3812752]
87. Chance B. On the mechanism of the reaction of cytochrome oxidase with oxygen. *Ann N Y Acad Sci*. 1975; 244:163–173. [PubMed: 237453]
88. Bassnett S, Reinisch L, Beebe DC. Intracellular pH measurement using single excitation-dual emission fluorescence ratios. *Am J Physiol*. Jan.1990 258:C171–8. [PubMed: 2301564]
89. Efimov IRR, Salama JMG. AHA abstract: Optical maps of intracellular [ca<sup>2+</sup>]<sub>i</sub> transients and action potentials from the surface of perfused guinea pig heart. *Circulation*. 1994; 90:1. [PubMed: 8025982]
90. Johnson PL, Smith W, Baynham TC, Knisley SB. Errors caused by combination of Di-4 ANEPPS and Fluo3/4 for simultaneous measurements of transmembrane potentials and intracellular calcium. *Ann Biomed Eng*. 1999; 27:563–571. [PubMed: 10468240]
91. Choi BR, Salama G. Simultaneous maps of optical action potentials and calcium transients in guinea-pig hearts: mechanisms underlying concordant alternans. *J Physiol*. Nov 15; 2000 529(Pt 1):171–88. [PubMed: 11080260]
92. Laurita KR, Singal A. Mapping action potentials and calcium transients simultaneously from the intact heart. *Am J Physiol Heart Circ Physiol*. May.2001 280:H2053–60. [PubMed: 11299206]
93. Pogwizd SM, Schlotthauer K, Li L, Yuan W, Bers DM. Arrhythmogenesis and contractile dysfunction in heart failure: Roles of sodium-calcium exchange, inward rectifier potassium current, and residual beta-adrenergic responsiveness. *Circ Res*. Jun 8.2001 88:1159–67. [PubMed: 11397782]
94. Baartscheer A, Schumacher CA, Belterman CN, Coronel R, Fiolet JW. SR calcium handling and calcium after-transients in a rabbit model of heart failure. *Cardiovasc Res*. Apr 1.2003 58:99–108. [PubMed: 12667950]
95. van Borren MM, den Ruijter HM, Baartscheer A, Ravesloot JH, Coronel R, Verkerk AO. Dietary Omega-3 Polyunsaturated Fatty Acids Suppress NHE-1 Upregulation in a Rabbit Model of Volume- and Pressure-Overload. *Front Physiol*. 2012; 3:76. [PubMed: 22485092]
96. Dillon S, Morad M. A new laser scanning system for measuring action potential propagation in the heart. *Science*. 1981; 214:453–6. [PubMed: 6974891]
97. Efimov I, Salama G. The future of optical mapping is bright: RE: review on: “Optical Imaging of Voltage and Calcium in Cardiac Cells and Tissues” by Herron, Lee, and Jalife. *Circ Res*. May 11.2012 110:e70–1. [PubMed: 22581923]
98. Coates CG, Denvir DJ, McHale NG, Thornbury KD, Hollywood MA. Optimizing low-light microscopy with back-illuminated electron multiplying charge-coupled device: enhanced sensitivity, speed, and resolution. *J Biomed Opt*. Nov-Dec;2004 9:1244–52. [PubMed: 15568946]
99. Lee P, Bollensdorff C, Quinn TA, Wuskell JP, Loew LM, Kohl P. Single-sensor system for spatially resolved, continuous, and multiparametric optical mapping of cardiac tissue. *Heart Rhythm*. Sep.2011 8:1482–91. [PubMed: 21459161]
100. Albeanu DF, Soucy E, Sato TF, Meister M, Murthy VN. LED arrays as cost effective and efficient light sources for widefield microscopy. *PLoS One*. 2008; 3:e2146. [PubMed: 18478056]

101. Holman B. LED light source: major advance in fluorescent microscopy. *Biomed Instrum Technol.* 2007; 41:4.
102. Salzberg BM, Kosterin PV, Muschol M, Obaid AL, Romyantsev SL, Bilenko Y, et al. An ultra-stable non-coherent light source for optical measurements in neuroscience and cell physiology. *J Neurosci Methods.* Jan 30.2005 141:165–9. [PubMed: 15585300]
103. Aanhaanen WT, Boukens BJ, Sizarov A, Wakker V, de Gier-de VC, van Ginneken AC, et al. Defective Tbx2-dependent patterning of the atrioventricular canal myocardium causes accessory pathway formation in mice. *J Clin Invest.* 2011; 121:534–544. [PubMed: 21266775]
104. Jalife J, Morley GE, Tallini NY, Vaidya D. A fungal metabolite that eliminates motion artifacts. *J Cardiovasc Electrophysiol.* Dec.1998 9:1358–62. [PubMed: 9869535]
105. Liu Y, Cabo C, Salomonsz R, Delmar M, Davidenko J, Jalife J. Effects of diacetyl monoxime on the electrical properties of sheep and guinea pig ventricular muscle. *Cardiovascular Research.* Nov.1993 27:1991–1997. [PubMed: 8287408]
106. Fedorov VV, Lozinsky IT, Sosunov EA, Anyukhovskiy EP, Rosen MR, Balke CW, et al. Application of blebbistatin as an excitation-contraction uncoupler for electrophysiologic study of rat and rabbit hearts. *Heart Rhythm.* May.2007 4:619–26. [PubMed: 17467631]
107. Kettlewell S, Walker NL, Cobbe SM, Burton FL, Smith GL. The electrophysiological and mechanical effects of 2,3-butane-dione monoxime and cytochalasin-D in the Langendorff perfused rabbit heart. *Exp Physiol.* Mar.2004 89:163–72. [PubMed: 15123545]
108. Biermann M, Rubart M, Wu J, Moreno A, Josiah-Durant A, Zipes DP. Effects of cytochalasin D and 2,3-butanedione monoxime on isometric twitch force and transmembrane action potentials in isolated canine right ventricular trabecular fibers. *J Cardiovasc Electrophysiol.* 1998; 9:1348–1357. [PubMed: 9869534]
109. Straight AF, Cheung A, Limouze J, Chen I, Westwood NJ, Sellers JR, et al. Dissecting temporal and spatial control of cytokinesis with a myosin II inhibitor. *Science.* Mar 14.2003 299:1743–7. [PubMed: 12637748]
110. Lou Q, Li W, Efimov IR. The role of dynamic instability and wavelength in arrhythmia maintenance as revealed by panoramic imaging with blebbistatin vs. 2,3-butanedione monoxime. *Am J Physiol Heart Circ Physiol.* Jan 1.2012 302:H262–9. [PubMed: 22037192]
111. Brack KE, Narang R, Winter J, Ng GA. The mechanical uncoupler blebbistatin is associated with significant electrophysiological effects in the isolated rabbit heart. *Exp Physiol.* May.2013 98:1009–27. [PubMed: 23291912]
112. Mironov SF, Vetter FJ, Pertsov AM. Fluorescence imaging of cardiac propagation: spectral properties and filtering of optical action potentials. *Am J Physiol Heart Circ Physiol.* Jul.2006 291:H327–35. [PubMed: 16428336]
113. Laughner JI, Ng FS, Sulkin MS, Arthur RM, Efimov IR. Processing and analysis of cardiac optical mapping data obtained with potentiometric dyes. *Am J Physiol Heart Circ Physiol.* Oct 1.2012 303:H753–65. [PubMed: 22821993]
114. Venkatachalam KL, Herbrandson JE, Asirvatham SJ. Signals and signal processing for the electrophysiologist: part II: signal processing and artifact. *Circ Arrhythm Electrophysiol.* Dec. 2011 4:974–81. [PubMed: 22203662]
115. Laughner JI, Gong Y, Filas BA, Zhang S, Efimov IR. Structured light imaging of epicardial mechanics. *Conf Proc IEEE Eng Med Biol Soc.* 2010; 2010:5157–60. [PubMed: 21095816]
116. Prinzen FW, Hunter WC, Wyman BT, McVeigh ER. Mapping of regional myocardial strain and work during ventricular pacing: experimental study using magnetic resonance imaging tagging. *J Am Coll Cardiol.* May.1999 33:1735–42. [PubMed: 10334450]
117. Meier GD, Bove AA, Santamore WP, Lynch PR. Contractile function in canine right ventricle. *Am J Physiol.* Dec.1980 239:H794–804. [PubMed: 7446754]
118. Villarreal FJ, Lew WY, Waldman LK, Covell JW. Transmural myocardial deformation in the ischemic canine left ventricle. *Circ Res.* Feb.1991 68:368–81. [PubMed: 1991344]
119. Gaudette GR, Todaro J, Krukenkamp IB, Chiang FP. Computer aided speckle interferometry: a technique for measuring deformation of the surface of the heart. *Ann Biomed Eng.* Sep.2001 29:775–80. [PubMed: 11599585]



120. Laughner JI, Zhang S, Li H, Shao CC, Efimov IR. Mapping cardiac surface mechanics with structured light imaging. *Am J Physiol Heart Circ Physiol*. Sep 15.2012 303:H712–20. [PubMed: 22796539]
121. Kong W, Ideker RE, Fast VG. Intramural optical mapping of V(m) and Ca(i)2+ during long-duration ventricular fibrillation in canine hearts. *Am J Physiol Heart Circ Physiol*. Mar 15.2012 302:H1294–305. [PubMed: 22268104]
122. Seo K, Inagaki M, Nishimura S, Hidaka I, Sugimachi M, Hisada T, et al. Structural heterogeneity in the ventricular wall plays a significant role in the initiation of stretch-induced arrhythmias in perfused rabbit right ventricular tissues and whole heart preparations. *Circ Res*. Jan 8.2010 106:176–84. [PubMed: 19893014]
123. Bourgeois EB, Bachtel AD, Huang J, Walcott GP, Rogers JM. Simultaneous optical mapping of transmembrane potential and wall motion in isolated, perfused whole hearts. *J Biomed Opt*. Sep. 2011 16:096020. [PubMed: 21950934]
124. Deisseroth K, Feng G, Majewska AK, Miesenbock G, Ting A, Schnitzer MJ. Next-generation optical technologies for illuminating genetically targeted brain circuits. *J Neurosci*. Oct 11.2006 26:10380–6. [PubMed: 17035522]
125. Miller G. Optogenetics. Shining new light on neural circuits. *Science*. Dec 15.2006 314:1674–6. [PubMed: 17170269]
126. Nagel G, Ollig D, Fuhrmann M, Kateriya S, Musti AM, Bamberg E, et al. Channelrhodopsin-1: a light-gated proton channel in green algae. *Science*. Jun 28.2002 296:2395–8. [PubMed: 12089443]
127. Nagel G, Szellas T, Huhn W, Kateriya S, Adeishvili N, Berthold P, et al. Channelrhodopsin-2, a directly light-gated cation-selective membrane channel. *Proc Natl Acad Sci U S A*. Nov 25.2003 100:13940–5. [PubMed: 14615590]
128. Boyden ES, Zhang F, Bamberg E, Nagel G, Deisseroth K. Millisecond-timescale, genetically targeted optical control of neural activity. *Nat Neurosci*. Sep.2005 8:1263–8. [PubMed: 16116447]
129. Arrenberg AB, Stainier DY, Baier H, Huisken J. Optogenetic control of cardiac function. *Science*. Nov 12.2010 330:971–4. [PubMed: 21071670]
130. Jia Z, Valiunas V, Lu Z, Bien H, Liu H, Wang HZ, et al. Stimulating cardiac muscle by light: cardiac optogenetics by cell delivery. *Circ Arrhythm Electrophysiol*. Oct.2011 4:753–60. [PubMed: 21828312]
131. Pinol RA, Bateman R, Mendelowitz D. Optogenetic approaches to characterize the long-range synaptic pathways from the hypothalamus to brain stem autonomic nuclei. *J Neurosci Methods*. Sep 30.2012 210:238–46. [PubMed: 22890236]
132. Zhang F, Wang LP, Boyden ES, Deisseroth K. Channelrhodopsin-2 and optical control of excitable cells. *Nat Methods*. Oct.2006 3:785–92. [PubMed: 16990810]
133. Neunlist M, Zou SZ, Tung L. Design and use of an “optrode” for optical recordings of cardiac action potentials. *Pflugers Archiv - European Journal of Physiology*. Apr.1992 420:611–617. [PubMed: 1614837]
134. Hooks DA, LeGrice IJ, Harvey JD, Smaill BH. Intramural multisite recording of transmembrane potential in the heart. *Biophys J*. 2001; 81:2671–2680. [PubMed: 11606280]
135. Pogwizd SM. Nonreentrant mechanisms underlying spontaneous ventricular arrhythmias in a model of nonischemic heart failure in rabbits. *Circulation*. Aug 15.1995 92:1034–48. [PubMed: 7543829]
136. Byars JL, Smith WM, Ideker RE, Fast VG. Development of an optrode for intramural multisite optical recordings of Vm in the heart. *J Cardiovasc Electrophysiol*. Nov.2003 14:1196–202. [PubMed: 14678134]
137. Kong W, Fakhari N, Sharifov OF, Ideker RE, Smith WM, Fast VG. Optical measurements of intramural action potentials in isolated porcine hearts using optrodes. *Heart Rhythm*. Nov.2007 4:1430–6. [PubMed: 17954403]
138. Janse MJ, Coronel R, Opthof T, Sosunov EA, Anyukhovskiy EP, Rosen MR. Repolarization gradients in the intact heart: transmural or apico-basal? *Prog Biophys Mol Biol*. May.2012 109:6–15. [PubMed: 22446189]

139. Antzelevitch C. Ionic, molecular, and cellular bases of QT-interval prolongation and torsade de pointes. *Europace*. Sep; 2007 9(Suppl 4):iv4–15. [PubMed: 17766323]
140. Kabra R, Singh JP. Catheter ablation targeting complex fractionated atrial electrograms for the control of atrial fibrillation. *Curr Opin Cardiol*. Jan.2012 27:49–54. [PubMed: 22123605]
141. Lau DH, Maesen B, Zeemering S, Verheule S, Crijns HJ, Schotten U. Stability of complex fractionated atrial electrograms: a systematic review. *J Cardiovasc Electrophysiol*. Sep.2012 23:980–7. [PubMed: 22554025]
142. Larsen AP, Sciuto KJ, Moreno AP, Poelzing S. The voltage-sensitive dye di-4-ANEPPS slows conduction velocity in isolated guinea pig hearts. *Heart Rhythm*. Sep.2012 9:1493–500. [PubMed: 22537886]
143. Fedorov VV, Ambrosi CM, Kostecki G, Hucker WJ, Glukhov AV, Wuskell JP, et al. Anatomic Localization and Autonomic Modulation of AV Junctional Rhythm in Failing Human Hearts. *Circulation Arrhythmia and electrophysiology*. Jun 6.2011
144. Lou Q, Fedorov VV, Glukhov AV, Moazami N, Fast VG, Efimov IR. Transmural Heterogeneity and Remodeling of Ventricular Excitation-Contraction Coupling in Human Heart Failure. *Circulation*. 2011; 123:1881–90. [PubMed: 21502574]

## Biographies



**Bas J Boukens** was born in Hoorn on december 7, 1982. After studying Biomedical Sciences at the University of Utrecht, he started to work on his PhD-thesis at the Heart Failure Research Center, University of Amsterdam. He defended his thesis with honours in 2012. Then he worked as a postdoctoral researcher at the department of Anatomy, Embryology and Physiology, University of Amsterdam. He is currently a research scientist at the department of Biomedical Engineering, Washington University, St Louis. The goal of his research is to understand the molecular mechanism underlying electrophysiological remodeling during heart disease.



Igor R. Efimov is the Lucy and Stanley Lopata Distinguished Professor of Biomedical Engineering, Professor of Radiology, Professor of Medicine (Cardiology), and Professor of Cell Biology & Physiology, Washington University in St. Louis, MO. He is the Director of the Cardiac Imaging Laboratory, an NIH-funded cardiovascular research and engineering

laboratory, which studies the physiological and biophysical mechanisms of cardiovascular disease and develops novel therapies for heart diseases. Dr. Efimov earned his M.Sc. and PhD from Moscow Institute of Physics and Technology in 1986 and 1992, respectively, and completed his postdoctoral training at the University of Pittsburgh (1992–1994). He served on the faculty of the Cleveland Clinic Foundation (1994–2000) and Case Western Reserve University (2000–2004) in Cleveland, OH, USA, prior to joining in 2004 the faculty of Washington University in St. Louis, MO, USA. Dr. Efimov is a Fellow of Heart Rhythm Society and American Heart Association. He is currently an Associate Editor of the American Journal of Physiology: Heart and Circulatory Physiology and an Associate Editor of IEEE Transactions in Biomedical Engineering.

Author Manuscript

Author Manuscript

Author Manuscript

Author Manuscript

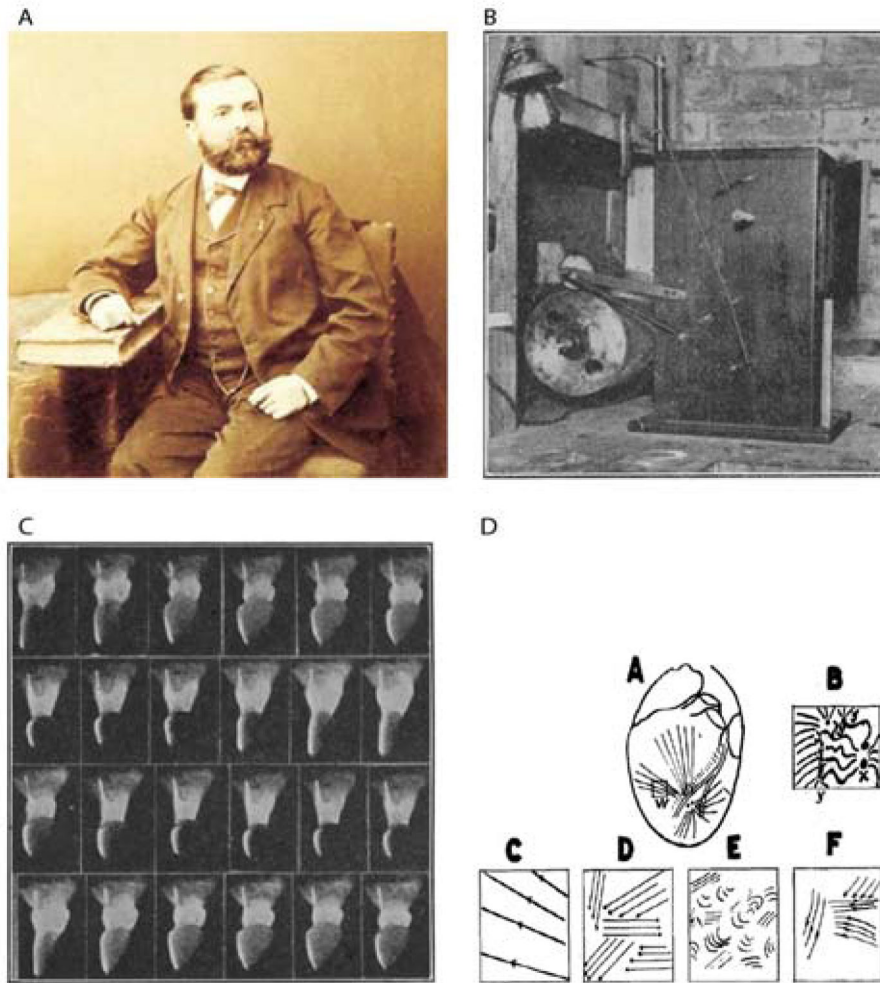


**Figure 1.** Early history of optocardiography started from work of Marey (A) whose cinematographic gun was used by Mines (B) to record contractions of a frog heart (C). Wiggers used fast film cinematography to analyze different phases of ventricular fibrillation (D).

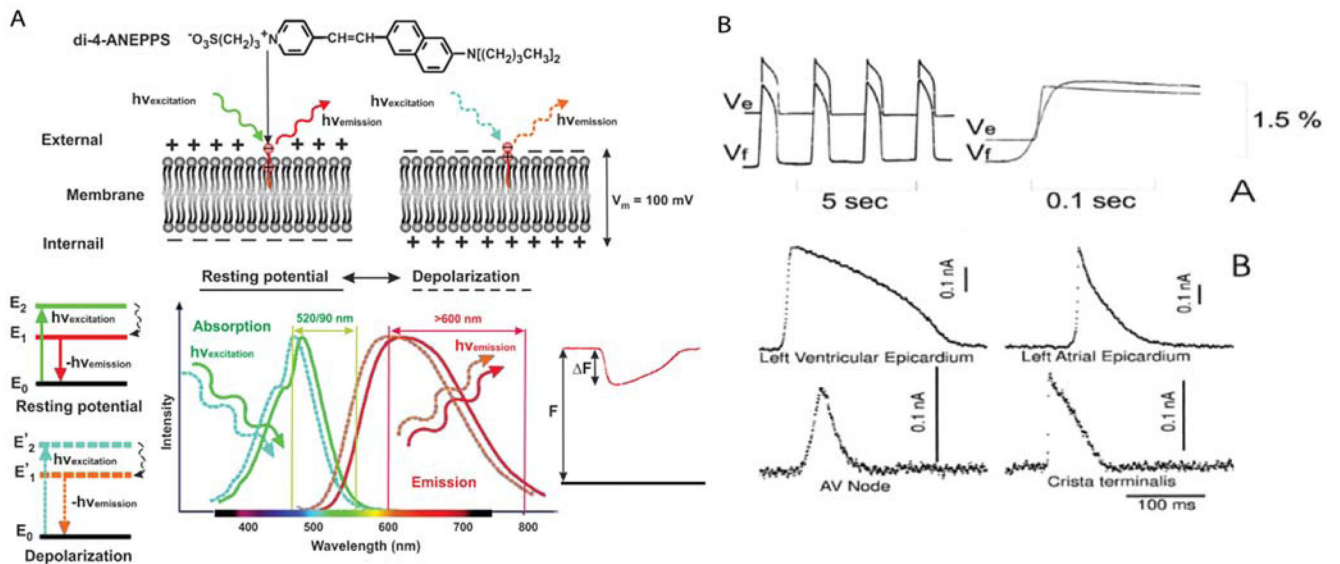


**Figure 2.**

Optical recording of cardiac action potentials using fluorescent dyes. A. The upper panel illustrates the conformation change of di-4-ANEPPS upon a change in membrane potentials. The lower panel shows the shift in emission spectrum results in a change in the amount of recorded fluorescence. B. The upper panel, Simultaneous fluorescent ( $V_f$ ) and microelectrode ( $V_e$ ) recordings of action potentials in the frog heart stained with Merocyanine-540. The lower panel, Optical recording of action potentials from different regions of the heart stained with di-4-ANEPPS: ventricular and atrial working myocardium, AV node, and Crista terminalis. Modified from Efimov [5].

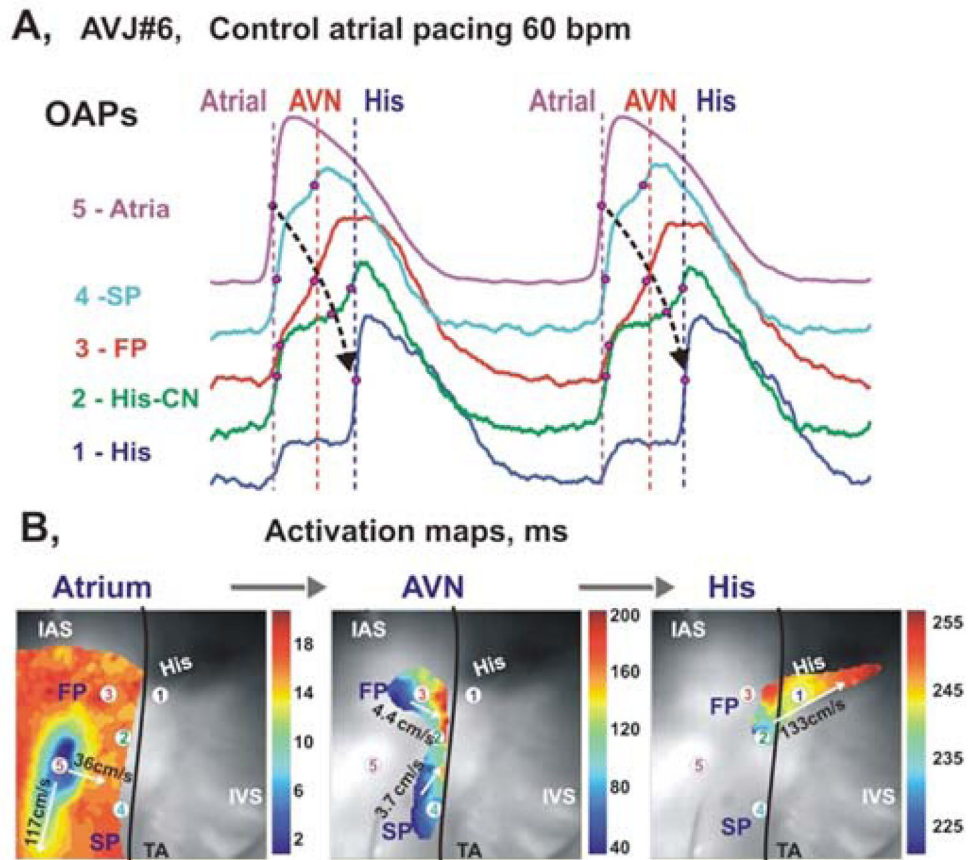


**Figure 3.**

Optical mapping of AVJ #6 during atrial pacing. Panel A: OAPs recorded from sites 1–5 in panels B, during atrial pacing at 60 bpm (CL=1000ms). Red dots on OAP upstrokes correspond to  $dV/dt$  peaks. Panel B: Separated atrial, AV nodal, and His bundle activation maps superimposed on the OFV ( $30 \times 30 \text{ mm}^2$ ). The black line demarcates the TA. Modified from Fedorov et al [143].

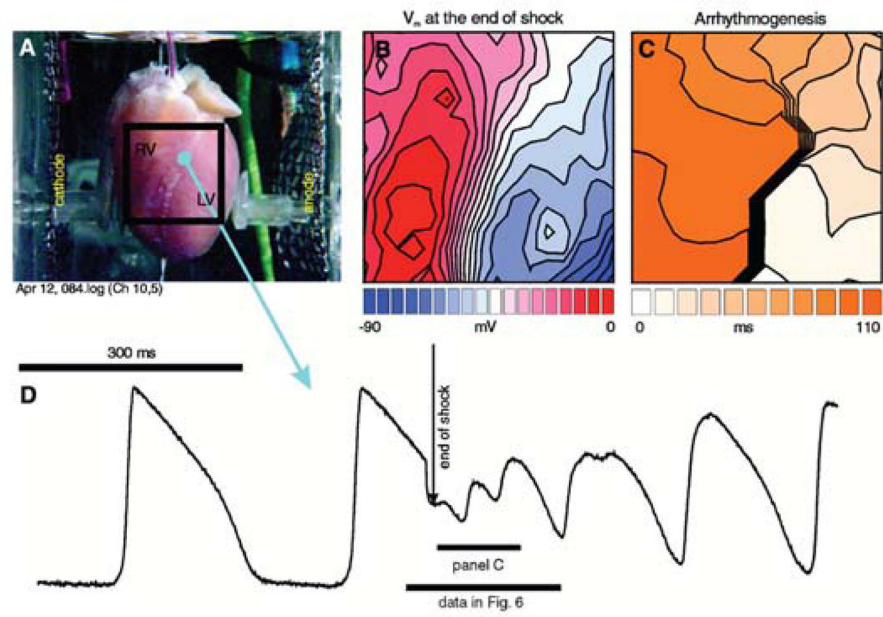


**Figure 4.** Optical imaging of shock-induced arrhythmogenesis and defibrillation. A, Preparation. B, Shock-induced polarization. C, Shock-induced conduction pattern. D, Optical recording of transmembrane potential during normal action potential, T-wave shock, and shock-induced arrhythmia. Modified from [32].

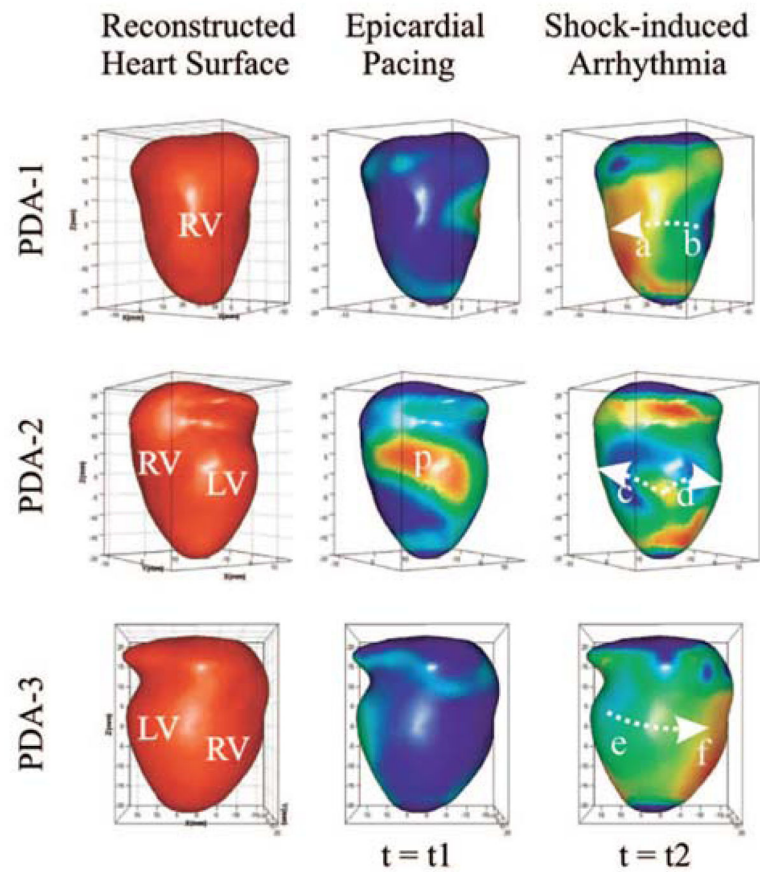


**Figure 5.**

Reconstructed heart surface and epicardial action potential texture mapping. (A) Left: reconstructed heart surface visualized from projections of PDA arrays. Middle: epicardial action potential texture mapping during epicardial pacing (p in PDA-2 projection is the pacing site). Right: epicardial action potential texture mapping during shock-induced ventricular tachycardia. Modified from Qu et al [144].



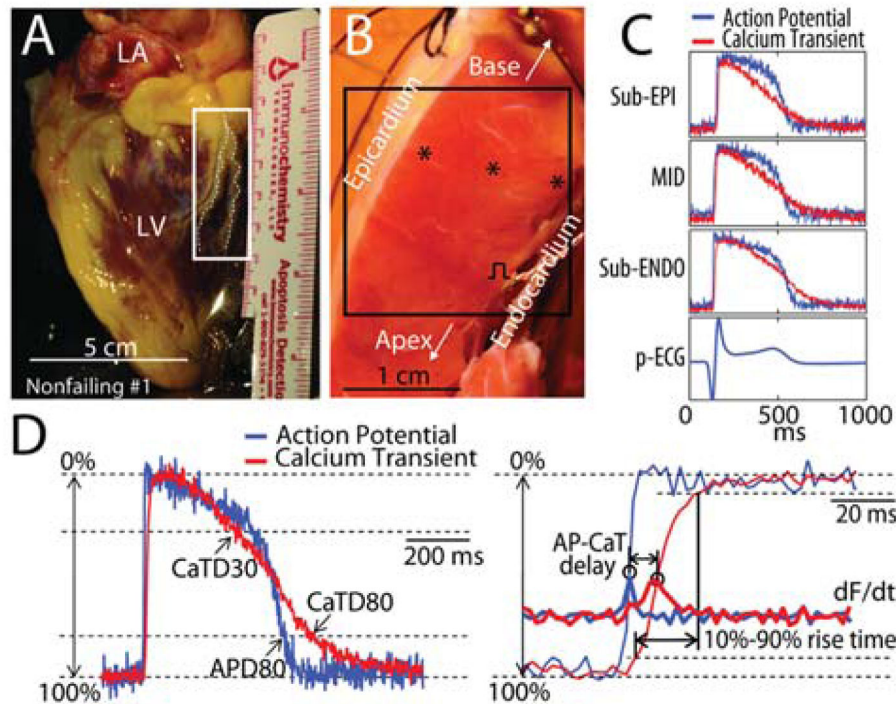


**Figure 6.**

Left ventricular wedge preparation and optical recordings of action potentials (AP) and calcium transients (CaT). (A) An explanted nonfailing human heart. The region indicated by white rectangle was dissected and cannulated for wedge preparation. (B) The left ventricular wedge preparation from the same heart. (C) Pseudo-ECG (p-ECG) and representative optical recordings of AP and CaT from locations within sub-endocardium (sub-ENDO), midmyocardium (MID), and sub-epicardium (sub-EPI), which are indicated by the black stars shown in the panel B. (D) Terminology. Left: superimposed AP and CaT with illustrations of AP duration at 80% repolarization (APD80), CaT duration at 30% and 80% recovery (CaTD30 and CaTD80). Right: Close-up view of upstrokes (thin lines), and the derivatives (thick lines, labeled as  $dF/dt$ ) with illustrations of AP-CaT delay and 10%–90% rise time of CaT. Modified from Lou et al [144].

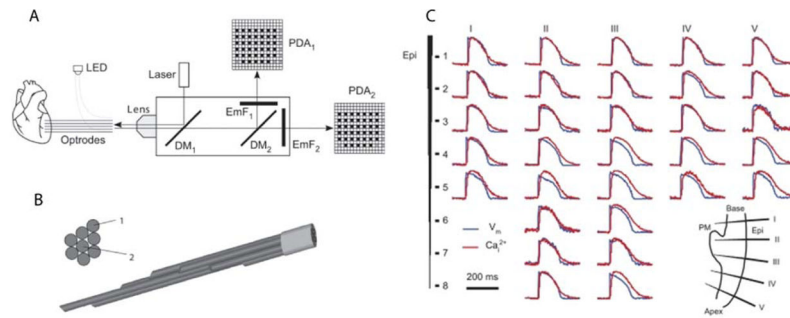


**Figure 7.**

A: schematic diagram of the optical system. LED, light-emitting diode; DM1 and DM2, first and second dichroic mirrors, respectively; EmF1, emission filter; PDA1 and PDA2, first and second photodiode arrays, respectively. B: cross-sectional and side views of the of the optrode tissue end. C: Intramural membrane voltage (Vm) and intracellular Ca<sup>2+</sup> (Ca<sup>2+</sup>) measured during regular rhythm. A: raw traces of Vm (blue) and Ca<sup>2+</sup> (red) from five optrodes. The inset in the bottom right corner schematically shows the optrode insertion sites. PM, papillary muscle; Epi, epicardium. Modified with permission from Kong et al. [121].